Supporting Information

Chirality enhancement in macro-chiral liquid crystal nanoparticles

Huanan Yu[1], Chris Welch[1], Wentao Qu[2], Christopher J Schubert[1], Feng Liu[2], Giuliano Siligardi[3], Georg H Mehl[1, 2]*

[1.] Department of Chemistry, University of Hull, Hull, HU6 7RX, United Kingdom
[2.] State Key Laboratory for Mechanical Behaviour of Materials, Xi'an Jiaotong University, Xi'an, P. R. China
[3.] Diamond Light Source, Harwell, Didcot OX11 0DE, United Kingdom

Contents

1. Methods

^{1}H-NMR was recorded at 400 MHz on a JEOL Eclipse 400 FT NMR spectrometer at ambient temperatures. All ^{1}H-NMR spectra were carried out using deuterated chloroform.

DSC data was collected on a Mettler-Toledo DSC822e in nitrogen against an indium standard.

High-resolution small-angle powder diffraction experiments were recorded on Beamlines BL16B1 at Shanghai Synchrotron Radiation Facility (SSRF). Samples were held in evacuated 1 mm capillaries. A modified Linkam hot stage with a thermal stability within 0.2 ℃ was used, with a hole for the capillary drilled through the silver heating block and mica windows attached to it on each side. q calibration and linearization were verified using several orders of layer reflections from silver behemate and a series of *n*-alkanes. A Pilatus detector was used for SAXS.

Mesophase behaviour of the samples was carried out using an Olympus BX51 polarising microscope. The microscope was equipped with a Mettler-Toledo FP900 heating stage.

UV/Vis spectra were recorded on Lambda 25 (Perkin-Elmer).

Circular dichroism (CD) spectroscopy experiments were performed at beamline B23 of the Diamond Light Source. An intense synchrotron-generated light beam of 0.8 x 1.5 mm^2 in diameter was used in the spectrometer, with the ability of samples to be scanned in xy plane and rotated. The beam was deflected vertically through the sample held horizontally between two quartz glass windows in a Linkam hot stage.

TEM were conducted by a JEOL 2010 high resolution with EDS capability and a Gatan Ultrascan 4000 camera for excellent image quality.

2. Experimental section

The synthesis of mesogenic ligand and the 1-hexanethiol functionalized gold nanoparticles has been described in Ref.[1-3] All nanoparticles were synthesized according to Supporting Information Scheme S1. All NP-LC mixtures were prepared by mixing specific weighed ratio of NPs or **L2** in mesogen **L1** or 5CB. From 1.0 wt% up to 6.5 wt% of NPs in mesogen **L1** were mixed in dichloromethane by stirring. Thereafter, the solvent was completely evaporated in an oven at 70 ℃ overnight. The Cano-wedge cell was purchased from Japan (KCRK-03, E.H.C., Tokyo, Japan) and the known tan $\theta = 0.0083$ is used to calculate the helical twisting power later. The homeotropic cell was purchased from Japan (KSHH-25/A107P1NSS, E.H.C., Tokyo, Japan) and the known cell gap = 25 μm is used to calculate the helical pitch. On a heating stage with temperature higher than the isotropic transition temperature of host LC (85 ℃), the cell gap was filled with NP-LC mixtures by capillary force and the cell was left for another 2 hours before OPM observation.

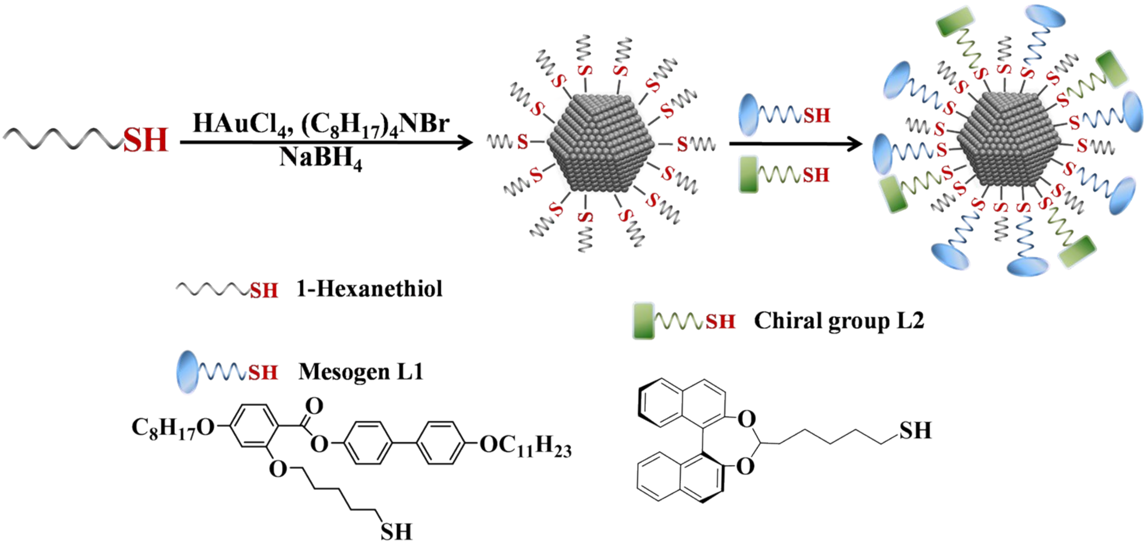

Scheme S1 Synthetic route of ChirAuLC.

Detailed synthetic information: Solution A was prepared by dissolving **L2** (10.0 mg, 0.02 mmol) and mesogen **L1** (40.0 mg, 0.06 mmol) in DCM (5 mL). Solution B was prepared by dissolving 1-hexanethiol capped AuNPs (13.25 mg) into DCM (10 mL). Then solution A and B were mixed in a 25 mL flask. The mixture was stirred at 25 ℃ under nitrogen for 5 days. The solvent was evaporated under reduced pressure to 2 mL. Ethanol (20 mL) was added to the crude product. The solution was sonicated and centrifuged using ethanol for 4 times (5000 rpm, 20 min). Finally, the product was dried in a *vacuum* oven. For the preparation of AuNPs linked with only **L2**, the method was similar to the above.

3. Calculations on the number of ligands on NPs and X-ray diffraction results

Table S1 Average NP core diameter (nm), number of Au atoms, number of ligands, average molecular weight (MW) of **ChirAuNP1** and **ChirAuLC1**.

NPs	NP Core Diameter (nm)	Number of Au Atoms	Number of Ligands	Molecular Weight (MW)
ChirAuNP1	1.87±0.31	211	28 **L2**, 25 1-hexanethiol.	56448.1 g/mol
ChirAuLC1	1.87±0.31	211	9 **L2**, 22 1-hexanethiol, 22 **L1**.	63164.6 g/mol

Table S2 Experimental and calculated *d*-spacings and diffraction intensities of **ChirAuNP2**, measured at 30 °C, including structure factor phase angles. The parameters in this columnar phase are a = 7.42 nm, b = 6.30 nm and γ = 77.1°.

(*hk*)	q	d_{exp}	d_{cal}	Iq^2
(10)	0.8682	7.24	7.23	4.9%
(01)	1.0226	6.14	6.14	100%
(11)	1.4820	4.24	4.24	2.5%
(2$\bar{2}$)	2.3585	2.66	2.65	2.5%
(13)	3.3869	1.86	1.86	2.8%

Table S3 Experimental and calculated *d*-spacings and diffraction intensities of **ChirAuLC2**, measured at 200 °C, including structure factor phase angles. The parameters are a = 6.98 nm, b = 5.93 nm and γ = 76.9°.

(*hk*)	q	d_{exp}	d_{cal}	I	Iq^2
(10)	0.9241	6.80	6.80	100%	100%
(2$\bar{2}$)	2.5139	2.50	2.50	0.6%	4.6%
(03)	3.2612	1.93	1.93	0.2%	2.8%

Table S4 Elemental analysis results of **ChirAuNP1** and **ChirAuLC1**.

NPs	C	H	N	S
ChirAuNP1	26.00%	2.61%	-	3.88%
ChirAuLC1	29.30%	3.54%	-	2.51%

The number of Au atoms in one single AuNPs is determined based on the formula:

$$N_{Au} = \frac{4 \times \pi \times R^3}{3 \times v_g} = \frac{4 \times \pi \times D^3}{8 \times 51}$$

R-radius of AuNPs (Å); D-diameter of AuNPs (Å); v_g-volume of gold atom (vg = 17 Å); 1 Å = 0.1 nm.

Based on TEM picture in Figure S3a, the average diameter of Au core is 1.9 nm.

$$N_{Au} = \frac{4 \times \pi \times 19^3}{8 \times 51} = 211$$

So, the number of gold atoms per particle is $N_{Au/particle} = 211$.

According to the model developed by Gelbart et al[7], the number of thiol on gold surface is obtained by the formula:

$$N_{thiol} = \frac{4 \times \pi \times R^2}{21.4} = \frac{\pi \times D^2}{21.4} = 53$$

In the ^{1}H NMR spectra of **ChirAuLC1** (see Fig. S7a), the signals at $\delta = 3.80$ ppm (-CH_2-O-), $\delta = 1.00$-2.00 ppm (-CH_2-) and $\delta = 0.85$ ppm (-CH_3-) can be used to estimate the molar ratio of **L1**, **L2** and 1-hexanethiol ($\text{Int}_{\delta = 3.80} : \text{Int}_{\delta = 1.00\text{-}2.00} : \text{Int}_{\delta = 0.85} = 6.00 : 52.64 : 9.08$). The molar ratio of **L1**, **L2** and 1-hexanethiol is 1 : 0.44 : 1.03. Combined with the number of thiol per particle 53, there are 22 **L1**, 9 **L2** and 22 1-hexanethiol on per NP.

The molecular weight of total number of gold atoms is 41567.6;

The molecular weight of total ligands on per NP is 21597.0;

The molecular weight of per particle is 63164.6.

In a similar calculation on **ChirAuNP1** ($\mathrm{Int}_{\delta} = {}_{1.00\text{-}2.00}$: $\mathrm{Int}_{\delta\,=\,0\cdot 85}$ = 3.00 : 21.00 in Fig. S7c), there are 28 **L2** and 25 1-hexanethiol on per NP and the molecular weight of per particle is 56448.1.

Table S5 Experimental and calculated *d*-spacings and diffraction intensities of **ChirAuNP1**, measured at 220 ℃, including structure factor phase angles. A columnar phase with *p*2 lattice is observed and the parameters are a = 4.20 nm, b = 3.14 nm, γ = 86.1°.

(*hk*)	***q***	d_{exp}	d_{cal}	Iq^2
(01)	2.0026	3.14	3.13	100%
(11)	2.5830	2.44	2.44	4.8%
(20)	3.0017	2.11	2.11	6.3%
(2$\bar{2}$)	4.8569	1.29	1.30	2.2%

If Bragg equation were used, the position of the diffuse maximum next to (10) corresponds to a *d*-spacing of c = 4.22 nm. However, in dense, disordered particle systems, the correlation function maximum is usually asymmetric, and as a guide, ～10% should be added to the “Bragg” value when estimating the average particle distance, giving a value of ～4.642 nm. This is likely to correspond to the average Au NP distance along the columns. In this module, the cell volume of single Au NP is $V_{xrd} = a\ b\ c\ \sin\gamma = 61.07\ \mathrm{nm}^3$.

Based on above calculation, there are 28 **L2** and 25 1-hexanethiol on single NP of **ChirAuNP1**. Thus the volume of single **ChirAuNP1** can be estimated as follows:

$$V1_{Au} = \frac{4 \times \pi \times 0.95^3}{3} = 3.59\ \mathrm{nm}^3$$

$$V2_{L2} = \frac{N \times M}{Na \times \rho} = \frac{28 \times 427}{6.02 \times 1.05 \times 100} = 18.91\ \mathrm{nm}^3$$

$$V3_{1\text{-}hexanethiol} = \frac{N \times M}{Na \times \rho} = \frac{25 \times 117}{6.02 \times 0.82 \times 100} = 5.93\ \mathrm{nm}^3$$

$$V_{ChirAuNP1} = V1 + V2 + V3 = 28.43\ \mathrm{nm}^3$$

Similarly, for **ChirAuLC1** (9 **L2**, 22 thiol and 22 **L1** on NPs), the volume of single NP was estimated as 36.81 nm^3.

$$V1_{Au} = \frac{4 \times \pi \times 0.95^3}{3} = 3.59\ \text{nm}^3$$

$$V2_{L2} = \frac{N \times M}{Na \times \rho} = \frac{9 \times 427}{6.02 \times 1.05 \times 100} = 6.08\ \text{nm}^3$$

$$V3_{1\text{-hexanethiol}} = \frac{N \times M}{Na \times \rho} = \frac{22 \times 117}{6.02 \times 0.82 \times 100} = 5.21\ \text{nm}^3$$

$$V4_{L1} = \frac{N \times M}{Na \times \rho} = \frac{22 \times 690}{6.02 \times 1.15 \times 100} = 21.93\ \text{nm}^3$$

$$V_{ChirAuLC1} = V1+V2+V3+V4 = 36.81\ \text{nm}^3$$

Table S6 Calculation results of ligands and cell volume for **ChirAuNP1** and **ChirAuLC1**.

Input of small sized AuNPs	
Average size from TEM for Au core	1.9 nm
Number of gold atom at interface	211
Number of thiol sites on Au surface	53
M.Wt. of total number of Au atoms	41567.6 g / mol
Calculated ligands on ChirAuNP1	
L2	28
1-Hexanethiol	25
M.Wt. of ligands on Au surface	14880.5 g / mol
Molecular weight of particles	56448.1 g / mol
Calculated ligands on ChirAuLC1	
L2	9
Mesogen **L1**	22
1-Hexanethiol	22
M.Wt. of ligands on Au surface	21597.0 g / mol
Molecular weight of particles	63164.6 g / mol
Input of XRD results for ChirAuNP1	
Average spacing of NPs along column (c)	4.22 nm
a	4.20 nm
b	3.14 nm
γ	86.1°
V_{xrd} (cell volume of single AuNP based on XRD results)	61.07 nm^3
$V_{\boldsymbol{ChirAuNP1}}$ (volume of single AuNP based on calculated ligands above)	28.43 nm^3
$V_{\boldsymbol{ChirAuLC1}}$ (volume of single AuNP based on calculated ligands above)	36.81 nm^3

4. Mesophase behaviour of mesogen L1 mixed with L2

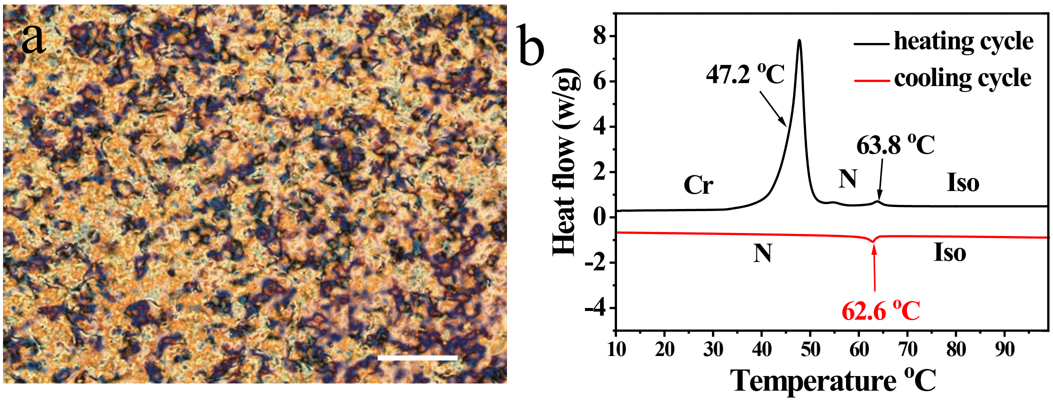

Fig. S1 (a) Optical polarizing microscopy (OPM) micrograph (90° crossed polarizer) of mesogen **L1** at 60 ℃ (x 100 μm), (b) DSC result of mesogen **L1**.

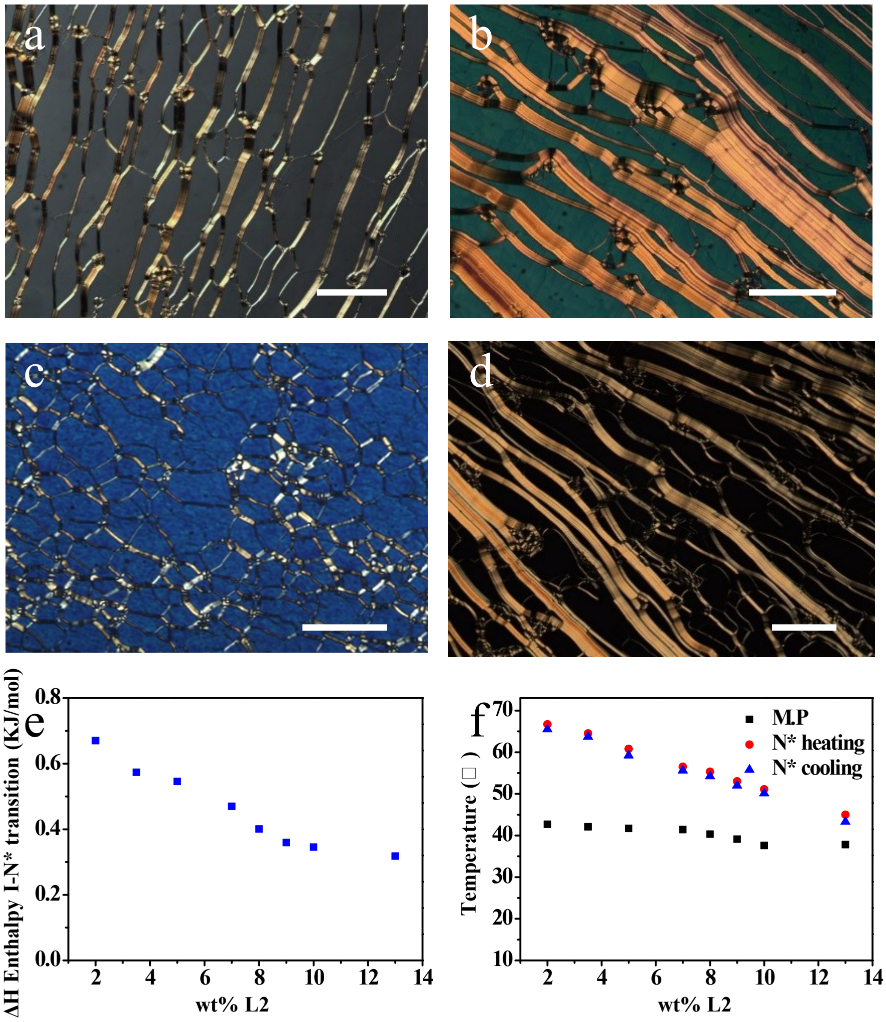

Fig. S2 OPM (90° crossed polarizer) micrographs of various weight percentage of **L2** in mesogen **L1** at 25 °C (a) 2.0 wt% (x 100 μm), (b) 3.5 wt% (x 100 μm), (c) 5.0 wt% (x 50 μm), (d) 7.0 wt% (x 100 μm), (e) Transition enthalpy of various mixtures, (f) Transition temperature of various mixtures (M.P: melting point. N* heating: transition temperature from chiral nematic phase to isotropic phase on heating. N* cooling: transition temperature from isotropic phase to chiral nematic phase on cooling).

5. TEM, XRD and UV-Vis tests on AuNP and ChirAuLC

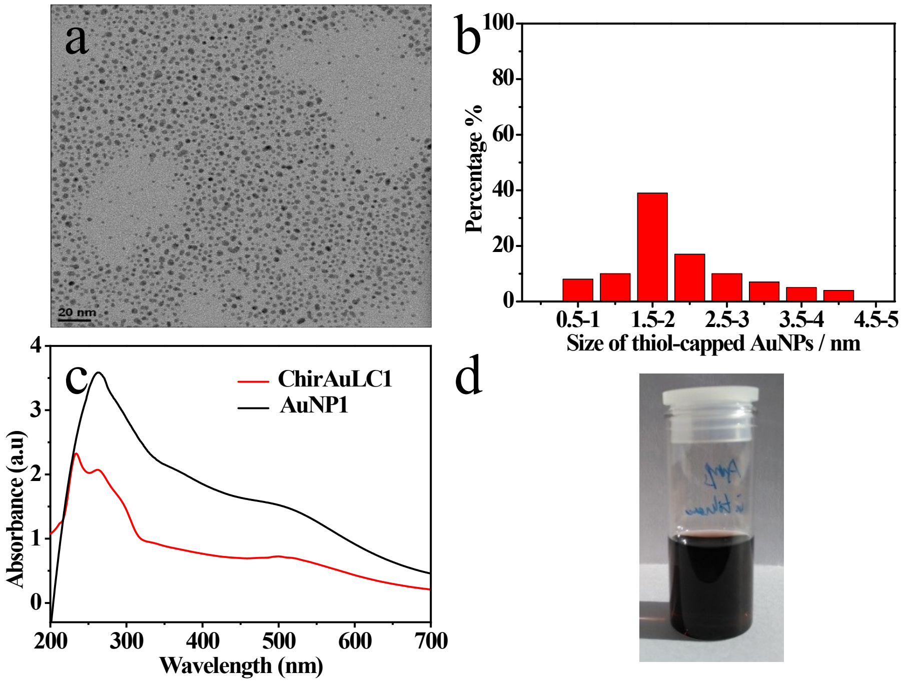

Fig. S3 (a) TEM picture of thiol-capped **AuNP1**, (b) Size distribution graph of **AuNP1**, (c) UV-Vis spectrums of **AuNP1** and **ChirAuLC1** (0.01 mol/L in DCM), (d) Photo picture of **AuNP1** in DCM.

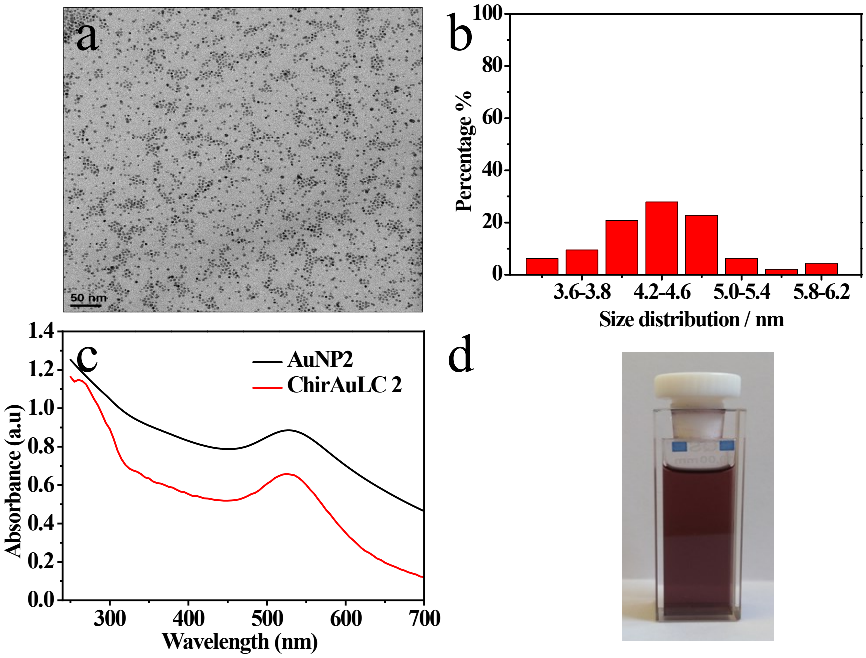

Fig. S4 (a) TEM picture of thiol-capped **AuNP2**, (b) Size distribution graph of **AuNP2**, (c) UV-Vis spectrums of **AuNP2** and **ChirAuLC2** (0.01 mol/L in DCM), (d) Photo picture of **AuNP2** in DCM.

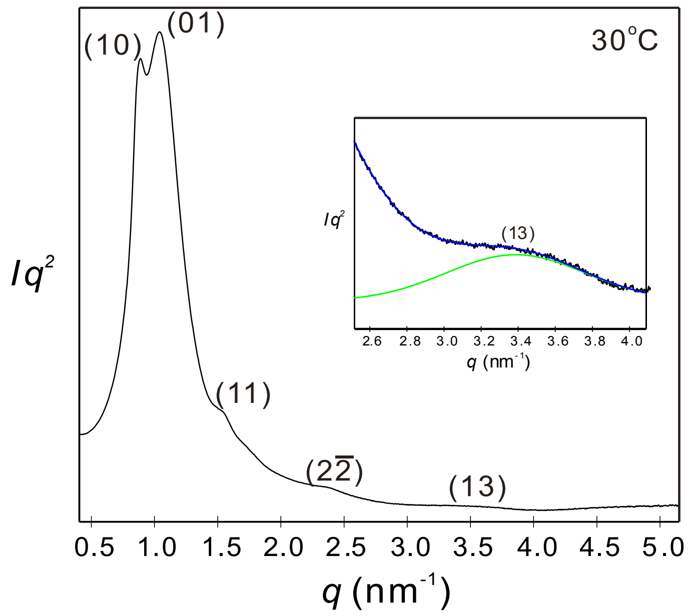

Fig. S5 SAXS result of **ChirAuNP2**. A columnar phase with *p*2 lattice is observed.

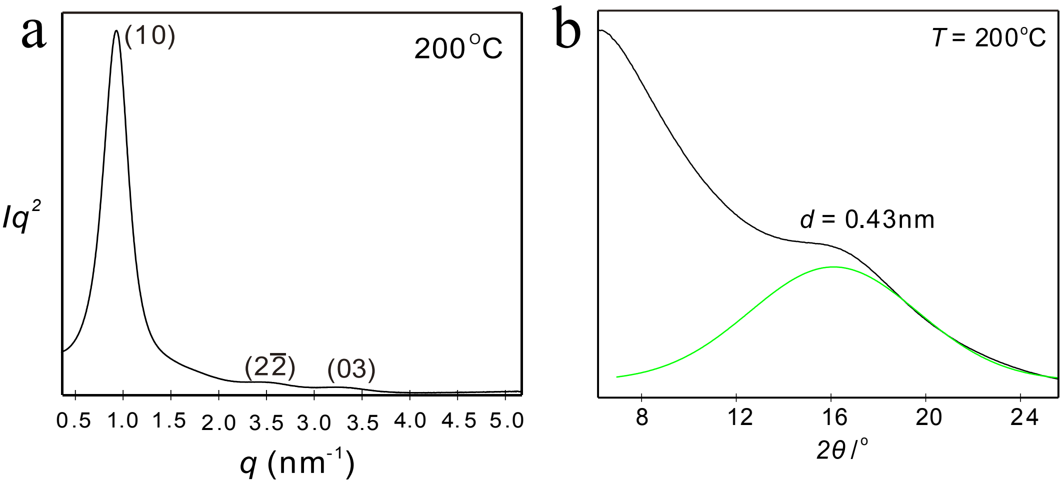

Fig. S6 (a) SAXS result of **ChirAuLC2**, (b) WAXS result of **ChirAuLC2**. For the WAXS result, a diffuse scattering peak can be observed, which shows the existence of liquid crystal phase.

6. ^{1}H-NMR, OPM and DSC study

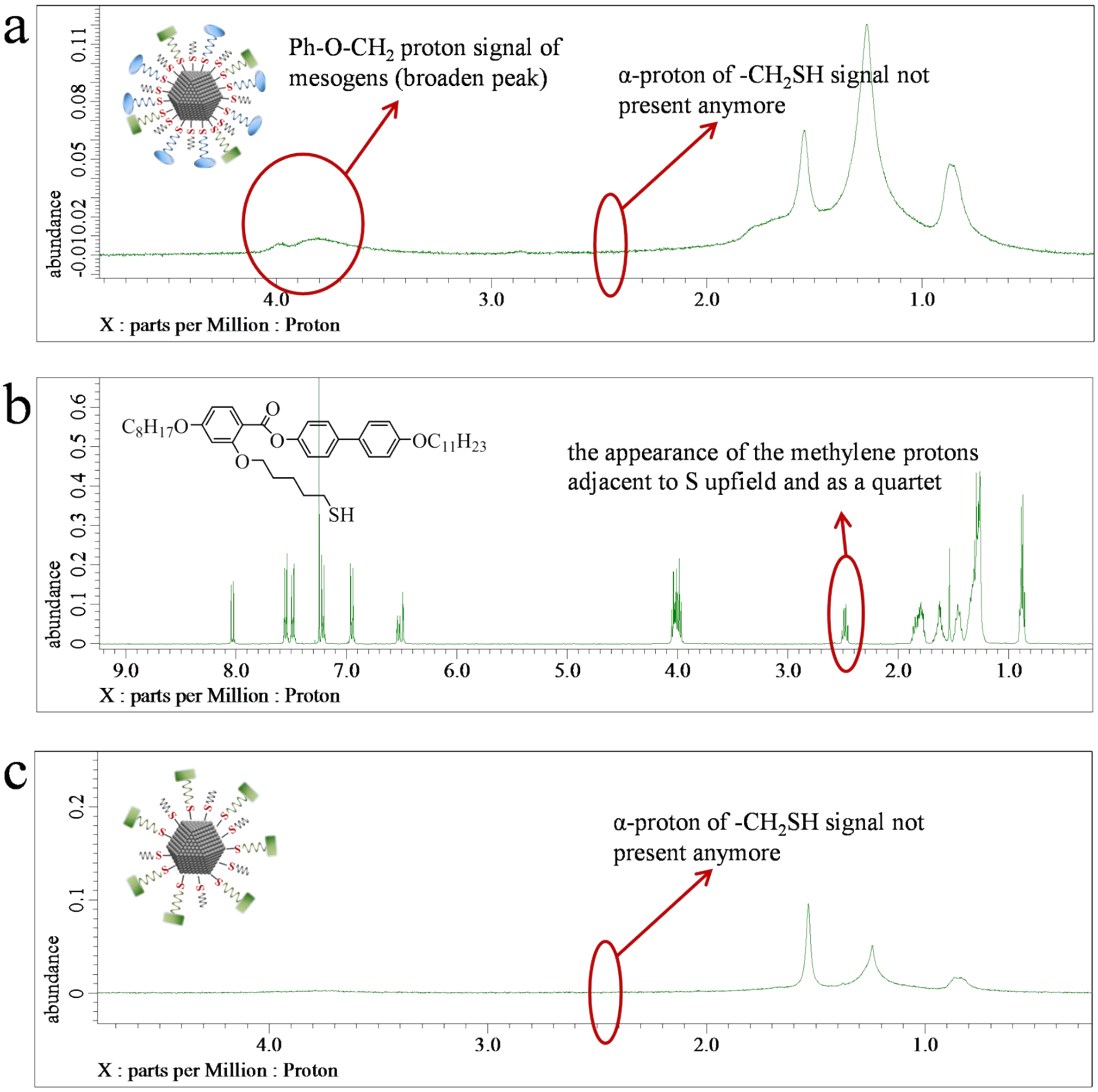

Fig. S7 (a) ^{1}H-NMR of **ChirAuLC1**, (b) ^{1}H-NMR of mesogen **L1**, (c) ^{1}H-NMR of **ChirAuNP1**.

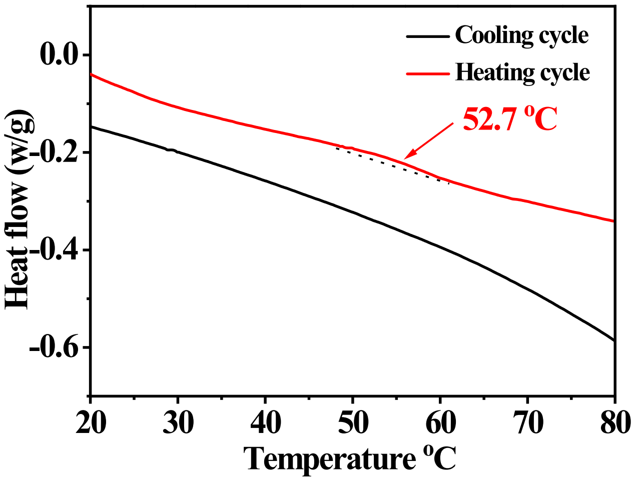

Fig. S8 DSC of **ChirAuLC1** recorded every 5.0 ℃/min upon heating and cooling.

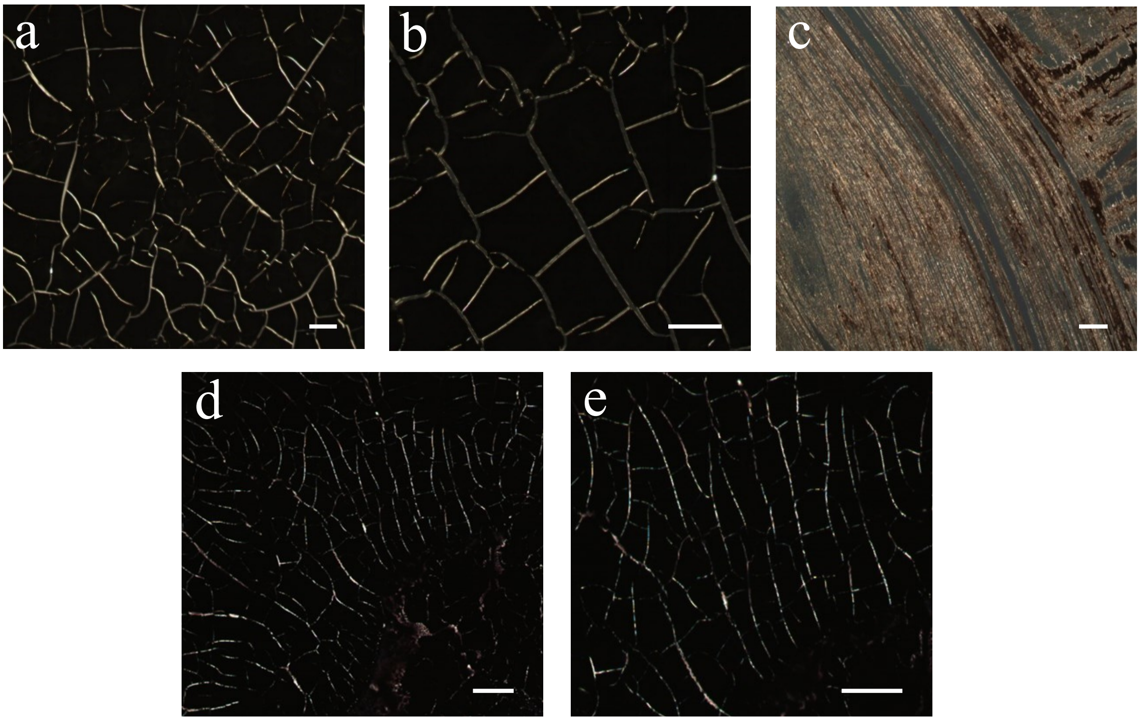

Fig. S9 OPM micrographs (90° crossed polarizer) (x 100 µm) of **ChirAuLC1** at room temperature in (a), (b), (c) After shearing, **ChirAuLC2** at room temperature in (d) and (e). The oily streaks in Fig. S9a and b disappeared at high temperature of 55 ℃. Static samples were observed as either a general birefringence with local scattering from line defects (believed to be disclinations), or in thicker samples a texture dominated by light scattering (due to the presence of dense disclinations). A translational oscillatory shearing motion to samples often results in typically 1-10 pm thickness. For **ChirAuLC1**, owing to the high solid gold in composite, at high shear rates, pure birefringence in the direction of flow is observed. When viewed in the optical microscope, the sample exhibits birefringence and or scattering where usually the light scattering is of sufficient intensity to limit transmitted-light microscopy to sample thicknesses < 15-20 pm.[8]

7. SRCD test on chiral NPs

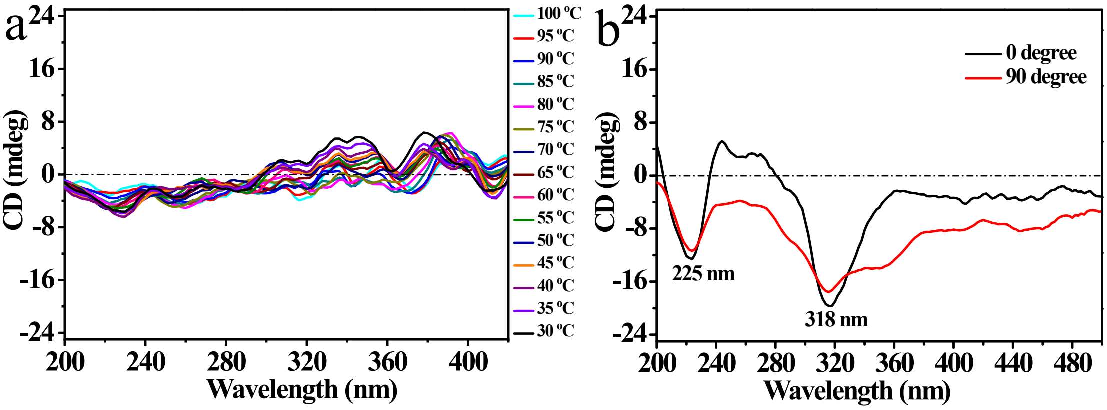

Fig. S10 SRCD spectra of (a) **ChirAuNP1** recorded every 5 ℃ upon cooling from 100 ℃ to 30 ℃, (b) **ChirAuLC1** recorded at 30 °C with the sample rotated around the centre of the light beam in the interval of 90°.

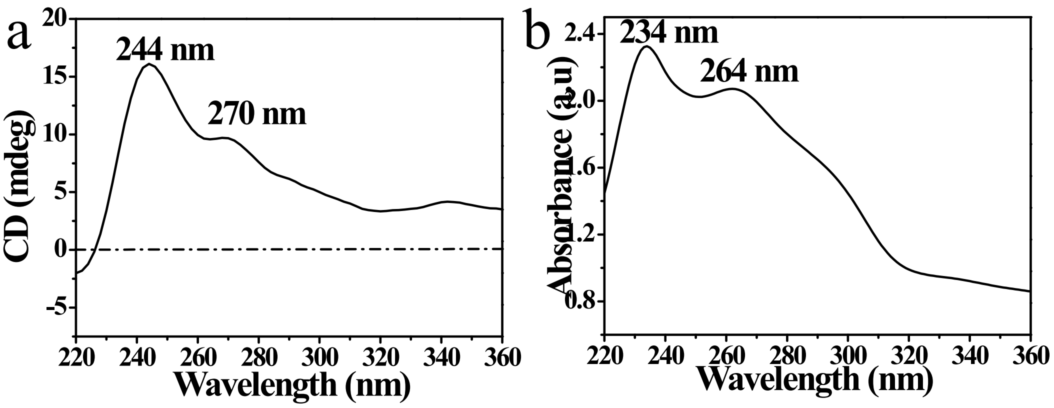

Fig. S11 (a) CD spectrum of **ChirAuLC1** in DCM, (b) UV-Vis of **ChirAuLC1** in DCM (0.01 mol/L).

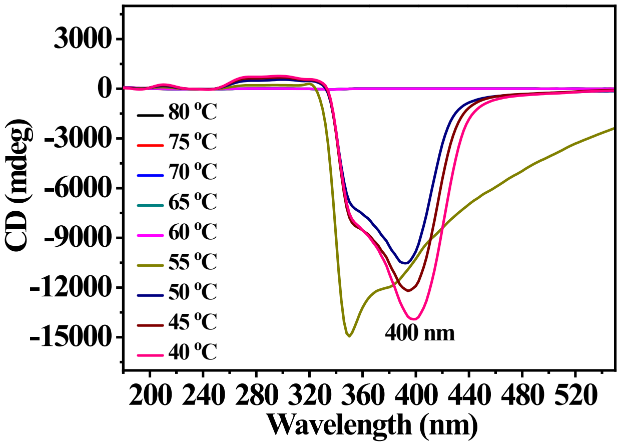

Fig. S12 SRCD spectra of mixture with 7.0 wt% **L2** in mesogen **L1** upon cooling from 80 °C to 40 °C. The significant CD intensity is attributed to the strong interference effects from linear dichroism in N* case.

8. TGA results of chiral NPs

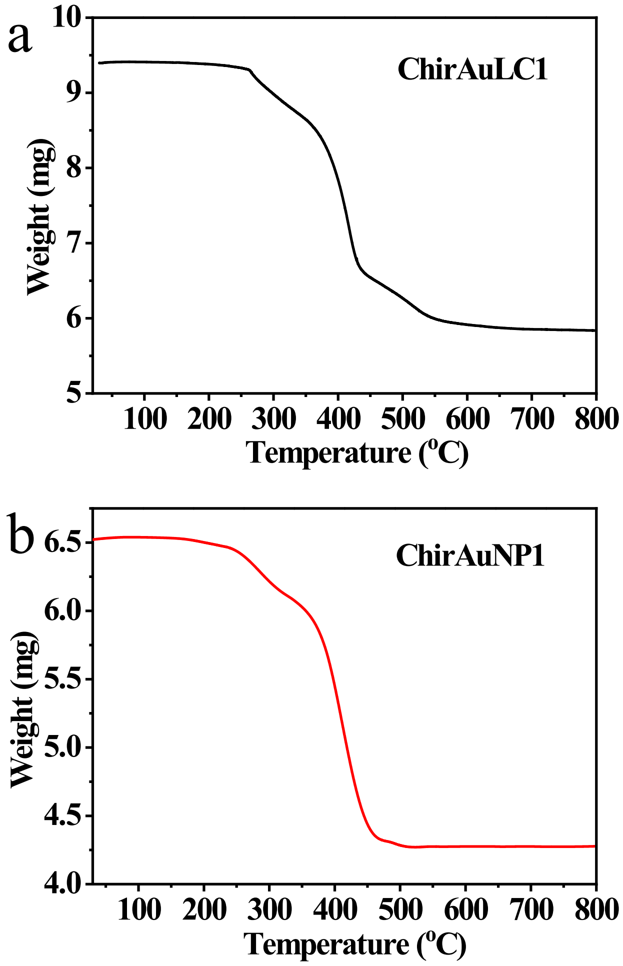

Fig. S13 TGA pictures of (a) **ChirAuLC1**, (b) **ChirAuNP1**.

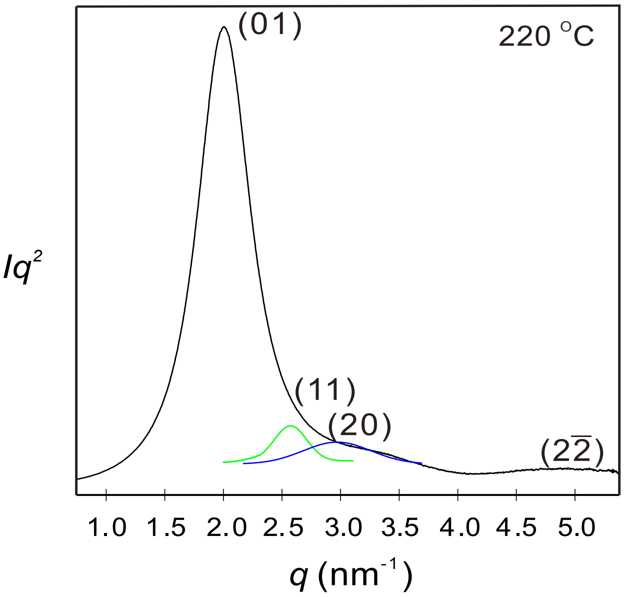

Fig. S14 SAXS result of **ChirAuNP1**.

9. OPM observation of chiral NPs mixed with L1 or 5CB

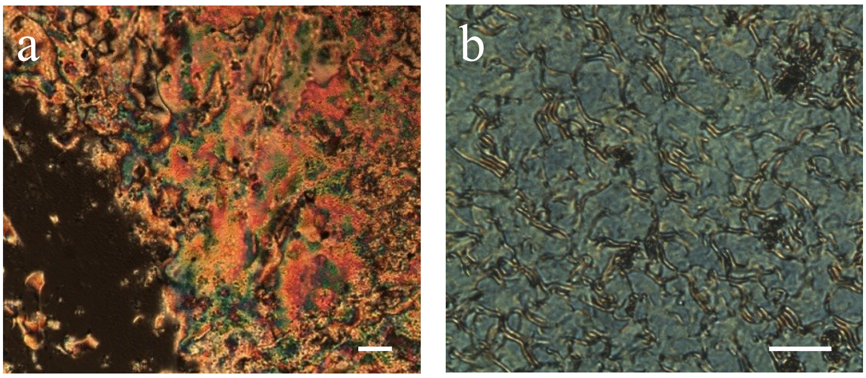

Fig. S15 OPM micrographs of mesogen **L1** at 25 ℃ doped with (a) 1.0 wt% **ChirAuLC1** (x 100 μm), (b) 5.0 wt% **ChirAuLC1** (x 25 μm).

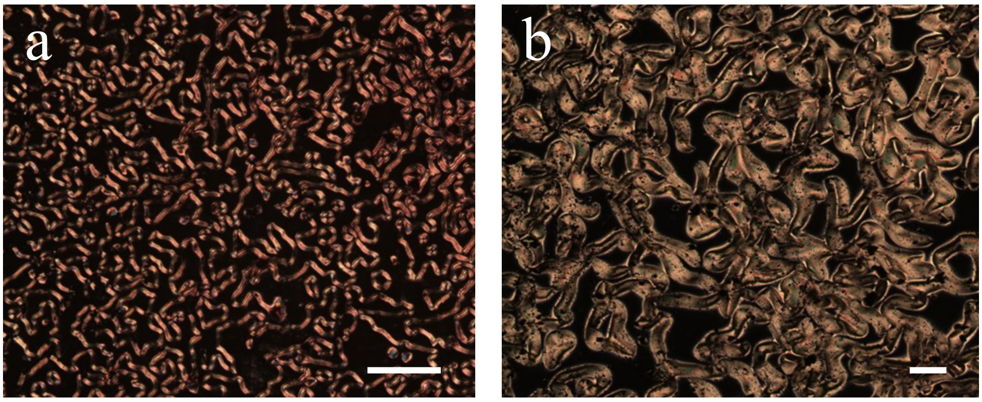

Fig. S16 The induced N* phase in 5CB after doping with (a) 3.0 wt% of **ChirAuNP2** (x 100 µm), (b) 3.0 wt% **ChirAuLC2** (x 100 µm).

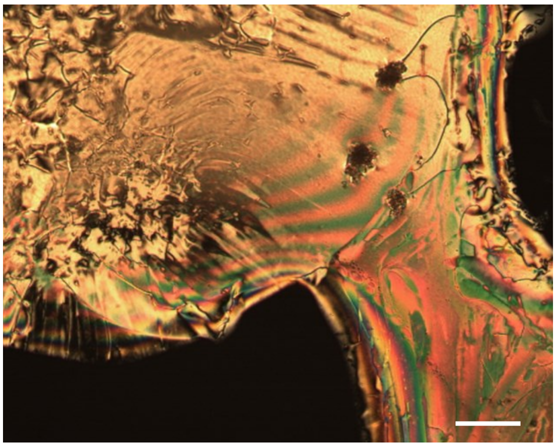

Fig. S17 Contact experiment of **ChirAuLC1** and mesogen **L1** (x 50 μm).

.

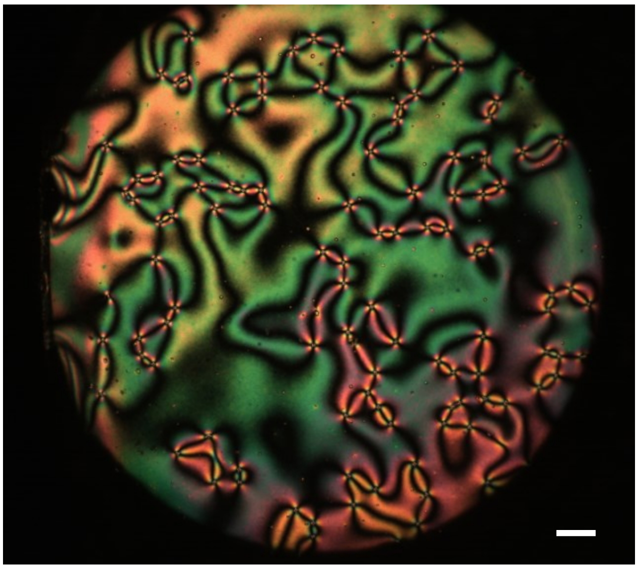

Fig. S18 OPM photo of 5CB shows the typical nematic phase (x 200 µm).

10. Additional information on chiral group L1

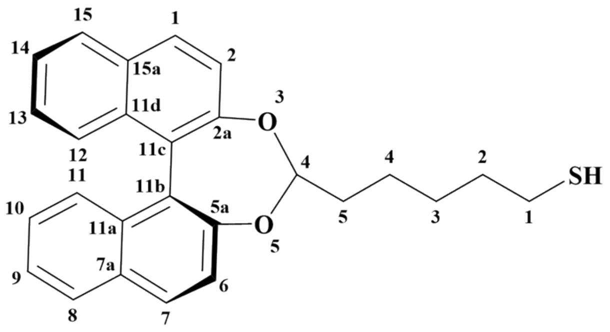

5-((11b*S*)-dinaphtho[2,1-*d*:1',2'-*f*][1,3]dioxepin-4-yl)pentane-1-thiol

Fig. S19 Chemical structure of binaphthol-based chiral groups (**L2**).

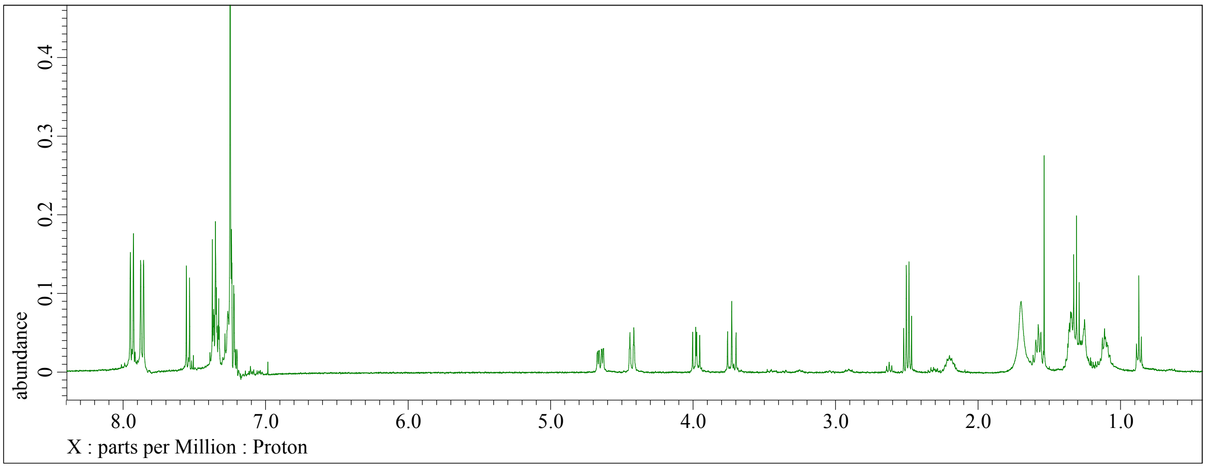

Fig. S20 ^{1}H NMR spectra of binaphthol-based chiral groups (**L2**).

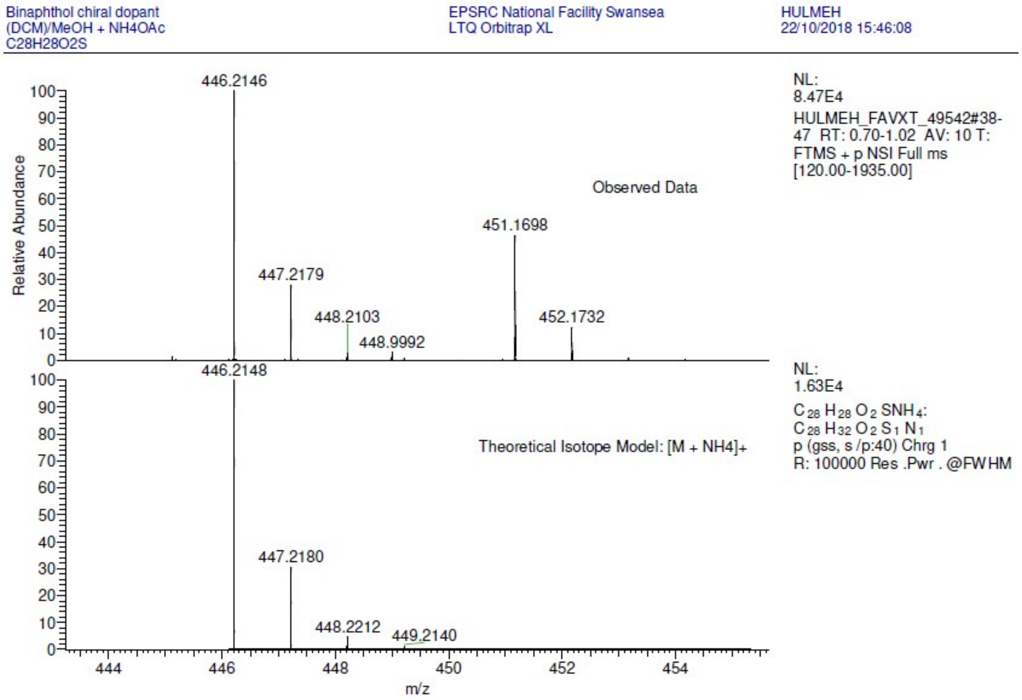

Fig. S21 Mass spectrum of binaphthol-based chiral groups (**L2**).

11. References

1 L. Cseh and G. H. Mehl, *Rev. Roum. Chim.,* 2013, **58**, 879-885.

2 M. Brust, M. Walker, D. Bethell, D. Schiffrin and R. Whyman, *J. Chem. Soc., Chem. Commun.,* 1994**,** 801.

3 M. Brust, J. Fink, D. Bethell, D. Schiffrin and C. Kiely, *J. Chem. Soc. Chem. Commun.,* 1995, 1655-1656.

4 J. Song, D. Kim and D. Lee, *Langmuir,* 2011, **27**, 13854-13860.

5 J. Dintinger, B. J. Tang, X. Zeng, F. Liu, T. Kienzler, G. H. Mehl, G. Ungar, C. Rockstuhl and T. Scharf, *Adv. Mater.,* 2013, **25**, 1999.

6 S. Umadevi, X. Feng and T. Hegmann, *Adv. Funct. Mater.,* 2013, **23**, 1393-1403.

7 D. V. Leff, P. C. Ohara, J. R. Heath and W. M. Gelbart, *J. Phys. Chem*., 1995, **99**, 7036-7041.

8 N. J. Alderman and M. R. Mackley, *Faraday Discuss. Chem. Soc*., 1985, **79**, 149-160.